Egypt.J.Chem. **Vol. 62**, No. 9. pp. 1603 - 1624 (2019)

Egyptian Journal of Chemistry
http://ejchem.journals.ekb.eg/

Synthesis of Some Triazole Schiff Base Derivatives and Their Metal Complexes under Microwave Irradiation and Evaluation of Their Corrosion Inhibition and Biological Activity

Ali M. Hassan[1], Bassem H. Heakal[2], Ahmed Younis[3], M. A. Bedair[1], Zaghloul. I. Elbialy[4] and M. M. Abdelsalam[4] *

[1]*Chemistry Dept., Faculty of Science, Al-Azhar University, Nasr City,11884, Cairo, Egypt*
[2]*Research Laboratory, Cairo Oil Refining Company, Mostorod, Qaliobia, Egypt.*
[3]*Green Chemistry Dept., National Research Centre, 33 El Bohouth st. (former EL Tahrir st.)-Dokki-Giza-Egypt-P.O.12622.*
[4]*Egyptian Organization for Standardization and Quality (EOS), Cairo, Egypt.*

TWO triazole Schiff base derivatives N-(furan-2-ylmethylene)-1H-1,2,4-triazole-3-amine (FTA), N-(thiophene-2-ylmethylene)-1H-1,2,4-triazole-3-amine (TTA) and their metal complexes Co(II), Ni(II), Cu(II) and Zn(II) were synthesized under microwave irradiation. The structure of these compounds has been investigated by using elemental analysis, FT-IR, UV-Vis spectrometric methods, magnetic susceptibility, mass spectra, NMR, ESR and thermal studies. The antimicrobial activities of the prepared ligands and their respective Zn (II) complexes were studied against the bacterial (positive and negative) grams and fungal strains. The inhibitive characteristics of Schiff base ligands on C-steel corrosion in hydrochloric acid were studied using weight loss measurements. The prepared Schiff base derivatives show high inhibition efficiency and their adsorption surface was found to obey Langmuir model. The data also revealed that FTA is less than TTA in terms of inhibiting efficiency.

Keywords: Microwave irradiation, Green chemistry, Thermal analysis, Corrosion inhibition, Biological activity.

Introduction

The microwave-assisted synthesis was acknowledged as a breakthrough in synthetic chemistry in recent years. This technique has overcome the certain back draws associated with conventional routes i.e. longer reaction time, slow rate of reaction, decreased yields and purity. Organic chemists have more opportunities to expand their synthetic avenues by applying microwave irradiation to a variety of organic reactions with improved results [1-4]. Utilization of Microwave heating (MWH) to prepare various refractory inorganic compounds and materials (double oxides, nitrides, carbides, semiconductors, glasses, ceramics, etc.) became common [5] as well as in organic processes [6] such as pyrolysis, esterification, and condensation reactions. Distinct aspects of microwave-assisted synthesis of various types of compounds and materials, in particular, organic [7] and organometallic compounds [8], applications in analytical chemistry and coordination chemistry have been described in recent excellent reviews[9]. It is well known that Schiff base compounds play an important role in the development of coordination chemistry so there has been considerable interest in the chemistry of metal complexes incorporating Schiff base [10-13]. The increased activity in this field may be explained to the striking structural feature, and its relation to their medicinal properties, their cytotoxic activity and their activity against bacteria, cancer and fungal [14-20]. It's also well known that many life

*Corresponding author e-mail: moatazmohamed@azhar.edu.eg
Received 20/3/2019; Accepted 8/4/2019
DOI: 10.21608/ejchem.2019.10834.1699

activities depend on the heterocyclic compounds, such as purine and pyrimidine bases unit of (DNA and RNA). Five-member N-heterocycle compounds, mainly tetrazole (CH_2N_4), Triazoles ($C_2H_3N_3$), and their substituted derivatives are a group of heterocyclic compounds that attracted researchers concern [21]. Corrosion inhibitors derived from Schiff bases containing triazoles and its derivatives had taken a lot of concerns in the last years [22-24]. These compounds can be categorized as environment-friendly inhibitors due to their strong chemical activities and limited toxicity. Plus, they have a special tendency towards metal surface enabling them to replace water molecules localized on the metal surface. In addition, they possess unshared electron pairs and considerable π-electrons on the nitrogen atoms that can interact with d-orbitals of iron metal to provide such a protective film preserving the metal from corrosion [25]. Encouraged by the previous reports and in continuation of our efforts in green chemistry [26-28], a new series of novel Schiff base ligands and their metal complexes were designed.

In the present study, Schiff base ligand and their metal complexes (Co^{II}, Ni^{II}, Cu^{II}, and Zn^{II}) were synthesized by microwave irradiation as a green approach. All resultant compounds were characterized spectroscopically using different techniques; thermogravimetric analysis and some thermo-kinetic parameter (ΔG, ΔH, and ΔS) were also calculated. The biological activities of some prepared compounds were also evaluated. We also investigated the efficiency of the synthesized triazole Schiff bases them as corrosion inhibitors by applying weight loss measurements on C-steel coupons in 1.0 M HCl solution.

Experimental

Materials and physical measurements

All organic solvents were purchased from commercial sources and used as received or dried using standard procedures unless otherwise stated. All chemicals were purchased from Merck, Aldrich or across and used without further purification, thin layer chromatography (TLC) was performed on precoated Merck 60 GF 254 silica gel plates with fluorescent indicator, detection by means of UV light at 254 and 360 nm. Melting point was measured by electrothermal apparatus, without correction the electronic absorption spectra (UV-Vis) of ligand and the metal complexes were obtained in DMF solvent from 900-200 nm range using Perkin-Elmer Lambda 35 UV/Vis Spectrophotometer fitted with a quartz cell of 1.0 cm path, the Fourier transform infrared spectra of the ligand, as well as the metal complexes dissolved in KBr, were recorded on Vertex 70 Analyzer, Bruker, USA from 4000–400 cm^{-1} and metal ions estimation was determined by complexometric titration using general lab glassware [29] at the faculty of science, Al-Azhar University, Cairo, Egypt. The magnetic susceptibility of the solid complexes was carried out at room temperature by the Gouy's technique for magnetic susceptibility instrument.

The thermogravimetric analyses (TGA) of the solid complexes were performed using the Schimadzu TG-50 thermogravimetric analyzer with a heating rate of of 10 °C/min under nitrogen atmosphere, in the range of 25—800 °C at the faculty of sciences, Cairo University. The thermodynamic activation parameters of decomposition processes of dehydrated complexes namely activation energy (E*), enthalpy (ΔH*), entropy (ΔS*) and Gibbs free energy change of the decomposition (ΔG*) are evaluated graphically by employing the Coats–Redfern [30] relation and Horowitz-Metzger [31]. The thermodynamic activation parameters for the thermal decomposition steps in complexes were calculated using the relationships:

$$\Delta H = E^* - RT \quad (1)$$

$$\Delta S^* = R[\ln(Ah/kT) - 1] \quad (2)$$

$$\Delta G^* = \Delta H^* - T\Delta S^* \quad (3)$$

Where *R* is the universal gas constant, *A* is the frequency factor, *h* is Plank's constant and *k* is Boltezmann constant.

The ESR spectra of the powdered Cu(II) sample were carried out on Bruker-EMX-(Xbands-9.7 GHZ) spectrometer with 100 KHZ frequency, microwave power 1.008 MW, modulation/ amplitude of 4 GAUSSES at National Center for Radiation Research and Technology, Egyptian Atomic Energy Authority. The elemental analysis for carbon, hydrogen, and nitrogen are carried out using a Flash 2000 organic Elemental Analyzer, Thermo, USA, the mass spectra were performed by an Agilent Technologies-6890N Network GC System and the biological activity evaluation of the synthesized ligands metal complexes was determined by using10 mg/ml solution in dimethyl sulfoxide (DMSO) at the Regional Center for Mycology and Biotechnology (RCMB) at Al-Azhar University [32]. The ^{1}HNMR and ^{13}C

spectra were recorded on an Agilent Technologies model spectrometer NMR400-mercury 400. ^{1}H spectra were run at 300 MHz and ^{13}C spectra were run at 75.46 MHz in dimethylsulphoxide (DMSO-d6). Tetramethylsilane (TMS) was used as an internal reference and chemical shifts are quoted in δ (ppm) at the Main Chemical Warfare Laboratories, Chemical Warfare Department, Ministry of Defense, Cairo, Egypt. Microwave-assisted reactions conducted on a commercially household microwave energy output 900 W, frequency 2450 MHz, manufactured by DAEWOO technologies Corporation, model: KOR-9G2B, Korai. Weight loss measurements were conducted using general lab glassware at the faculty of Science, Al-Azhar University, Cairo, Egypt.

Synthesis and preparation

Synthesis of the Schiff base Ligands (FTA and TTA)

An equimolar ratio (1:1) of 3-amino-1, 2, 4-triazole and appropriate aldehyde (furan-2-carboxaldehyde or thiophene-2- carboxaldehyde) was ground and mixed thoroughly in a grinder until it reached a satisfactory homogeneity. The reaction mixture was then transferred to a clean crucible and moisturized by adding drops of methanol as a solvent then transferred to the microwave oven thus irradiated and heated gradually by using on/off cycling to control the temperature. The reaction completed in a short time (3, 4 min) respectively with high yields (95, 89.1 %) respectively. The products were then recrystallized with hot methanol and finally dried under reduced pressure over anhydrous $CaCl_2$ in a desiccator. The progress of the reaction and purity of the product was monitored by TLC.

Preparation of the solid complexes

All the isolated solid complexes were prepared by mixing equimolar amounts of ligand (FTA or TTA) and metal (II) acetates [M = Co(II), Ni(II), Cu(II) and Zn(II)]. The reaction mixtures were then irradiated by microwave by adding drops of methanol. The reaction completed in a short time (4-6 min) with high yields (67-84 %). The obtained products were washed by hot methanol and ether then finally dried under reduced pressure over anhydrous $CaCl_2$ in a desiccator. The progress of the reaction and purity of the products were monitored by TLC. Table 1 shows the elemental analysis and physical properties of the Schiff base ligand and their metal complexes.

Corrosion Inhibition studies

Corrosion inhibition behavior of the two synthesized ligands (FTA) and (TTA) was evaluated on carbon steel specimens by using weight loss measurements as follows:

Carbon steel coupons used

The surface of the carbon steel coupons was abraded successively by different grade of metallographic emery papers until the surface appears free from any scratches and other apparent defects, then degreased with hot acetone, washed with distilled water and finally dried at room temperature. Tests were conducted on carbon steel coupons of the following composition: (0.11%C, 0.45% Mn, 0.04% P, 0.05% S, 0.25% Si, and the remained is Fe).

Concentration range of ligands and acid

The concentrations of the prepared ligands were 0.5×10^{-4} M, 0.75×10^{-4}M, 2.5×10^{-4} M, 5×10^{-4} M, and 7.5×10^{-4} M. All solutions were prepared using distilled water.

Weight loss measurement

The experiments were carried out using carbon steel coupons immersed in 1.0 M HCl solution in absence and presence of different concentrations of the two synthesized Schiff base inhibitors. Tests were conducted under total immersion conditions in 100 ml of the aerated test solutions. To determine weight loss with respect to time, test coupons were retrieved after 24 h immersion time, scrubbed with a bristle brush, washed, dried, and reweighed. The weight loss was taken as the difference between the initial and final weights of the coupons. Weight loss measurements were done at three different temperatures 30 °C, 40 °C and 50 °C.

Procedure for antibacterial activity

Antibacterial and Fungi studies

The Schiff base ligands (FTA), (TTA) and their respective Zn(II) complexes were tested and evaluated for their antimicrobial activity using the agar diffusion technique (Cooper, 1972) [32, 33]. 5 mg/ml solution in dimethyl sulfoxide was used. The tested organisms were Gram-negative bacteria (Escherichia Coli (RCMB 010052) ATCC 25955& Salmonella typhimurium RCMB 006 (1) ATCC 14028), Gram-positive bacteria (Bacillus subtilis, RCMB 015 (1) NRRL B-543& Staphylococcus aureus, RCMB010010) and fungi (Aspergillus flavus, RCMB 002008) & Candida albicans RCMB 005003 (1) ATCC 10231). The bacteria and fungi were maintained on nutrient agar medium and Czapeks Dox agar medium, respectively. DMF showed no inhibition zones.

TABLE 1. Melting points, yields, reaction time, analytical and physical properties of the prepared compounds.

Comp.	Molecular Formula	M.P °C	Yield %	Time min	Color	Elemental Analysis Calc. / (Found) %				M^+ Calc./ (Found)
						C	H	N	M	
FTA	$C_7H_6N_4O$	175	95	3	Beige	51.85 (52.50)	3.73 (3.80)	34.55 (33.51)	-	162.08 (162.05)
Co	$C_{11}H_{18}CoN_4O_8$	>360	74.91	5	Violet	33.60 (34.50)	4.61 (4.10)	14.25 (13.67)	14.99 (13.36)	393.22
Ni	$C_{18}H_{22}N_8NiO_8$	>360	73.77	5	Green	40.25 (40.03)	4.13 (4.60)	20.86 (20.95)	10.93 (11.90)	537.12
Cu	$C_{11}H_{16}CuN_4O_7$	>360	67.22	5	Deep Green	34.79 (35.20)	4.25 (3.92)	14.75 (15.60)	16.73 17.71	379.8
Zn	$C_{11}H_{16}N_4O_7Zn$	>360	77.77	6	White	34.62 (34.20)	4.23 (4.30)	14.68 (15.09)	17.13 (17.53)	381.65
TTA	$C_7H_6N_4S$	155	89.1	4	Brown	47.18 (48.11)	3.36 (3.63)	31.44 (31.27)	-	178.06 (178.03)
Co	$C_{18}H_{22}CoN_8O_6S_2$	>360	83.94	5	Violet	37.96 (38.70)	3.89 (3.30)	19.68 (20.20)	10.35 (11.65)	569.5
Ni	$C_{11}H_{18}N_4NiO_7S$	>360	77.61	5	Light . Green	32.30 (31.69)	4.44 (4.93)	13.70 (13.97)	14.35 (13.97)	409.04
Cu	$C_{11}H_{16}CuN_4O_6S$	>360	82.06	4	Deep . Green	33.37 (32.70)	4.07 (4.40)	14.15 (13.30)	16.05 (17.05)	395.88
Zn	$C_{11}H_{16}N_4O_6SZn$	265	71.21	5	White	33.22 (33.50)	4.06 (3.65)	14.09 (15.30)	16.44 (17.12)	397.71

The agar media were inoculated with different test microorganism. After 24 h of incubation at 37°C for bacteria and 48 h of incubation at 28°C for fungi, the diameter of inhibition zone (mm) was measured.

Results and Discussion

All compounds containing five or four-member rings with (-N- heterocycle), azomethine, oxygen and sulfur atom possess basic characteristics due to the presence of lone pair electron-donating character of the double bond of (-HC=N) and the capability to form metal complexes as illustrated in Schemes (1) and (2). The ligands FTA and TTA were prepared by the reaction of 3-amino-1,2,4-triazole and appropriate aldehyde (furan-2-carboxaldehyde and thiophene-2-carboxaldehyde) under microwave irradiation as an approach for green chemistry (Scheme 1, 2) all structures were confirmed based on the following techniques:

IR spectra

Table 2 shows the main IR bands displayed by FTA and TTA ligands and their complexes. The peaks due to (N-H), (C=N) and (N-N) of triazole moiety were showed at 3107, 1575 and 1088 cm^{-1} respectively in the IR spectra of the ligand. The structure of Schiff-base ligands was further confirmed due to The absence of aldehydic (CHO) and amino (NH_2) bands at 3325 and 1715 cm^{-1} respectively while the azomethine (-C=N) linkage appeared as a sharp band at 1619 cm^{-1} [34]. Actually, the bands due to vibration of various groups such as C=N (azomethine and triazole), NH, N-N, C-N, and C-H appear in the overlapping regions so it could not be assigned unequivocally. The IR spectra of metal complex confirm the involvement of the azomethine (C=N) where its band shifted to 1624–1600 while all

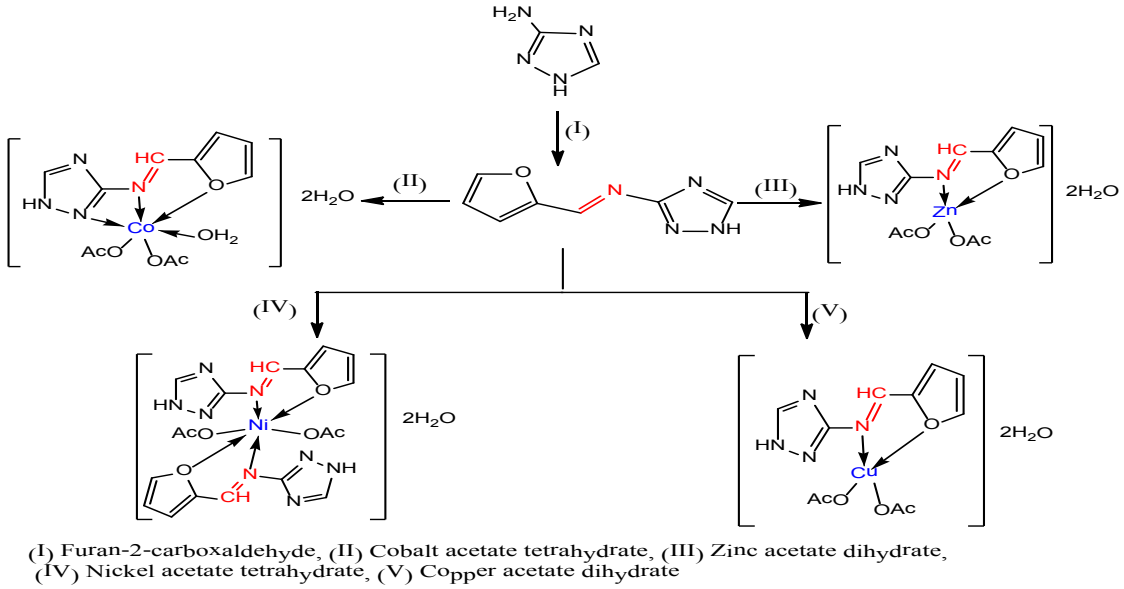

Scheme 1. Synthesis of FTA ligand and its metal complexes.

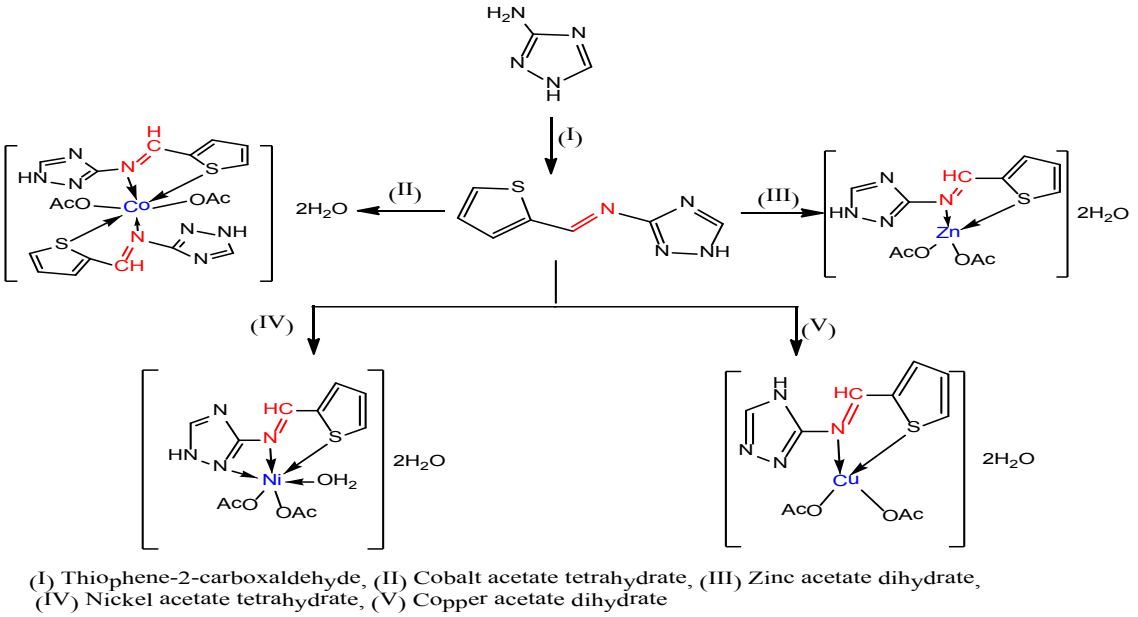

Scheme 2. Synthesis of TTA ligand and its metal complexes.

ligands showing IR spectral bands at 1610–1604 cm^{-1} by comparing the IR spectra of ligands and their metal complexes we concluded the following:

In the complexes of the triazoles (FTA and TTA) coordinate with the metal ions in di- and tridentate forming stable four or five-membered chelate rings around the metal ions. This various behavior of ligands can be explicated from the IR data set out in Table 2. The mode of bonding in complexes can be identified by comparing IR spectra of complexes with that of the related ligands as follows:

1) Vibration of (M–N) in all the metals (II) complexes, exhibited a new band 622–475 cm^{-1} proving the coordination of nitrogen of (azomethine and triazole) with the metal ions. However, the unchanged band of ν(N–N) mode at 1087-1015 cm^{-1} in the IR spectra of all the metal complexes evinces the triazole

ring nitrogen is not involved.

2) Appearance of new band in the spectra of metal complex at 455–421 cm^{-1} is assigned due to M–S Vibration [35] evinces the involvement and coordination of thienyl-S ring in the complexation phenomenon in addition to vibration of (C-S) in the spectra of the ligand TTA which appears at 969 cm^{-1} is shifted to high frequency at 999-967 cm^{-1} in the spectra of the metal (II) complexes of TTA confirm this coordination.
3) All other bands of all ligands and their corresponding metal complexes appeared at the same region without change.

Electronic spectra and magnetic properties

The electronic absorption spectra of the Schiff-base ligands and its complexes as shown in Table 3 were performed in dimethylformamide (DMF). The electronic spectra of the prepared ligands (FTA) and (TTA) showed three absorption bands at 360 -364 nm refers to n $\longrightarrow$ π^*, of C=N triazole and at 296-315 nm refers to π $\longrightarrow$ π^*, of C=N azomethane. The third band was at 244-254 nm refers to π $\longrightarrow$ π^*, of C=C aromatic rings. For cobalt (II) complexes: The electronic spectra of FTA and TTA cobalt complexes showed absorption bands at (450, 600) and (425, 635) nm assigned to ^4T_1g (F) $\rightarrow$ ^4T_1g(P) ^4T_1g (F)$\rightarrow$ ^4T_2g transitions are respectively. The observation of these bands suggests an octahedral configuration around Co (II) ion [36] and all the complexes are paramagnetic and the magnetic moment is (4.57-5.17) BM. For nickel (II) complexes: The electronic spectra of Ni complexes showed bands of appreciable intensity at (450, 655) and (475, 600) nm and assigned to $^3A_2g\rightarrow{}^3T_1g$ (P) $^3A_2g\rightarrow{}^3T_2g$ (F) for FTA and TTA, are respectively. The observation of these bands suggests an octahedral and the magnetic moment is (2.25-2.52) B.M. For copper (II) complexes: The electronic spectra of the copper complexes revealed bands of considerable intensity at (425, 575) and (470, 650) nm assigned to the transitions ($^2B_2 \rightarrow {}^2E$) assuming a tetrahedral configuration for FTA and TTA respectively, thus the prepared Cu-complexes are paramagnetic, the obtained magnetic moment value 1.90 and 1.97 B.M. For zinc complexes: the absorption bands at the range (425, 450) and (430, 475) nm for FTA and TTA in the electronic spectra of Zn (II) complex can be assigned to metal ligand (M $\rightarrow$L) transition and its positions in agreement with low-spin tetrahedral geometry for Zn (II) complexes.

Mass spectra of the Schiff base ligand

The mass spectrum of the **FTA** shows ion peak at m/e = 162 as the molecular peak due to ($C_7H_6N_4O$). The ion peak at m/e = 164.10 (3.34 %) is due to $M^+(C_7H_8N_4O)$, the ion peak at m/e = 135 (8.75 %) corresponds to $M^+(C_6H_5N_3O)$. The ion peak at m/e = 134 (51 %) corresponds to $M^+(C_7H_6N_2O)$. The ion peak at m/e = 121 (100 %) corresponds to $M^+(C_6H_6N_2O)$ which is the base peak. The ion peak at m/e = 95.06 (11.60 %) refers to $M^+(C_5H_5NO)$, while the ion peak at m/e = 84 (1.41 %) corresponds to $M^+(C_2H_4N_4)$, The ion peak at m/e = 69.04 (17.49 %) corresponds to $M^+(C_2H_3N_3)$ and the ion peak at m/e = 52.05 (28.86 %) corresponds to $M^+(C_4H_4)$. The fragmentation patterns of **FTA**, are shown in Scheme 3; Fig. 1. The MS of **TTA** shows ion peak at m/e = 178 as the molecular peak is due to ($C_7H_6N_4S$). The ion peak at m/e = 162 (100 %) is due to $M^+(C_5H_{14}N_4S)$ which is the base peak, while the ion peak at m/e = 167 (13 %) corresponds to $M^+(C_6H_7N_3S)$. The ion peak at m/e = 138 (3 %) corresponds to $M^+(C_6H_7N_3)$, while the ion peak at m/e = 113 (21 %) refers to $M^+(C_5H_7NS)$, while the ion peak at m/e = 96 (9 %) corresponds to $M^+(C_3H_4N_4)$, the ion peak at m/e = 84 (18 %) corresponds to $M^+(C_2H_4N_4)$, the ion peak at m/e = 52 (86 %) corresponds to $M^+(C_4H_4)$ and the ion peak at m/e = 45 (91%) corresponds to $M^+(C_2H_7N)$. The fragmentation patterns of **TTA**, are shown in Scheme 4; Fig. 2.

NMR Spectra

The ^{1}HNMR spectra of ligands FTA and TTA have been recorded in DMSO-d_6. The characteristic absorption ^{1}HNMR signals are represented in Fig. 3& 4. The ^{1}HNMR (DMSO) of FTA showed also peaks at δ = 6.72-6.73 ppm (t, 1H, furan C4-H), 7.30-7.338 ppm (dd, 1H, furan C3-H), 7.50-7.51 ppm (d, 1H, furan C5-H), 9.52 ppm (s, 1H, triazole C-H), 8.88 ppm (s, 1H, azomethine C-H), 13.75 ppm (s, 1H, triazole NH). The ^{1}HNMR (DMSO) spectra of the synthesized ligand (TTA) showed peaks at δ = 7.23 ppm (t, 1H, thiophene C4-H), 7.86 ppm (d, 1H, thiophene C3-H), 8.25 ppm (d, 1H, thiophene C5-H), 9.1 ppm (s, 1H, azomethine C-H), 9.32 ppm (s, 1H, triazole C-H), 13.98 ppm (d, 1H, triazole NH). The ^{13}CNMR spectra of the Schiff base ligand (FTA) and (TTA) were taken in DMSO-d6. The characteristic absorbtion^{13}CNMR signals are given in Fig. 5& 6. [37-39]. The ^{13}CNMR (DMSO) of the

TABLE 2. FT-IR of the prepared compounds.

Sym.	ν(OH), (H_2O)	ν(NH)	ν(C-H) Ar/Alph	ν(C=N) azomethane	ν(C=N) triazole	ν(C=C)	ν(OAc) as/s	ν(C-O)	ν(N-N)	Furan ring	ν(C-S)	ν(M-N)	ν(M-O)	ν(M-S)
FTA	-	3112	3028	1610	1526	1477	-	1338	1087	627 588	-	-	-	-
Co	3429 3338	3155	-	1617	1570	1548	1414	1341	1055	630, 540	-	615	448	-
Ni	3427	3150	-	1613	1581	1544	1415	1333	1058	623, 580	-	622	457	-
Cu	3333	3154	-	1615	1578	1550	1397	1339	1067	668 550	-	621	490	-
Zn	3397	3130	2939	1624	1591	1518	1428	1396	1069	620, 594	-	555	490	-
TTA	-	3128 3101	3037	1604	1533	1516	1482 1451	1361 1331	1047 1015	-	969	-	-	-
Co	3445	-	-	1601	1554	1490	1414	1341 1283	1050 1018	-	968	480	-	439
Ni	3444 3359	3154	-	1600	1554	1542	1415	1343	1050 1021	-	987	475	-	437
Cu	3429 3328		-	1600	1574	1480	1446 1413	1339	1050	-	970	492	-	-
Zn	3395	-	-	1610	1592	1517	1409	1336	1068	-	990	491	-	427

TABLE 3. Magnetic and spectral data of the Schiff base ligands and their metal complexes.

Comp.	λ_{max}, nm	Assignments	μ_{eff} (BM)	g⊥	g\\	gav	Suggested Structure
FTA	364 315 254	(n-π*, C=N), (π -π*, C=N), (π -π*, aromatic ring)	-	-	-	-	-
Co	450 600	^4T_1g (F) →^4T_1g(P) ^4T_1g (F)→^4T_2g	5.17	-	-	-	Octahedral
Ni	450 655	^3A_2g→^3T_1g (P) ^3A_2g→^3T_2g (F)	2.25	-	-	-	Octahedral
Cu	425, 575	$^2B_2$→^2E	1.90	2.19	2.03	2.14	Tetrahedral
Zn	425, 450	M →L	Di	-	-	-	Tetrahedral
TTA	360 296 244	(n-π*, C=N), (π -π*, C=N), (π -π*, aromatic ring)	-	-	-	-	-
Co	425 635	4T1g (F) →4T1g(P) ^4T_1g (F)→^4T_2g	4.57	-	-	-	Octahedral
Ni	475 600	3A2g→3T1g (P) 3A2g→3T2g (F)	2.52	-	-	-	Octahedral
Cu	470, 650	$^2B_2$→^2E	1.97	2.05	2.02	2.04	Tetrahedral
Zn	430, 475	M →L	Di	-	-	-	Tetrahedral

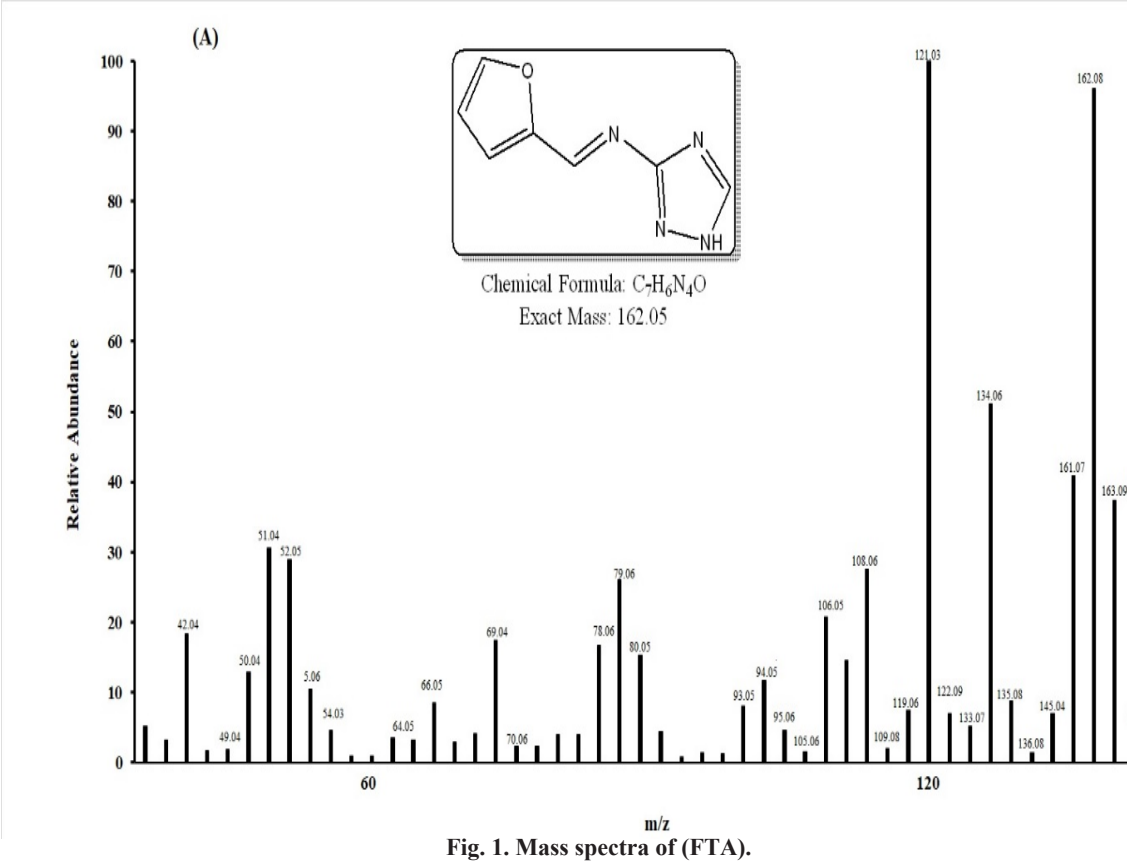

Fig. 1. Mass spectra of (FTA).

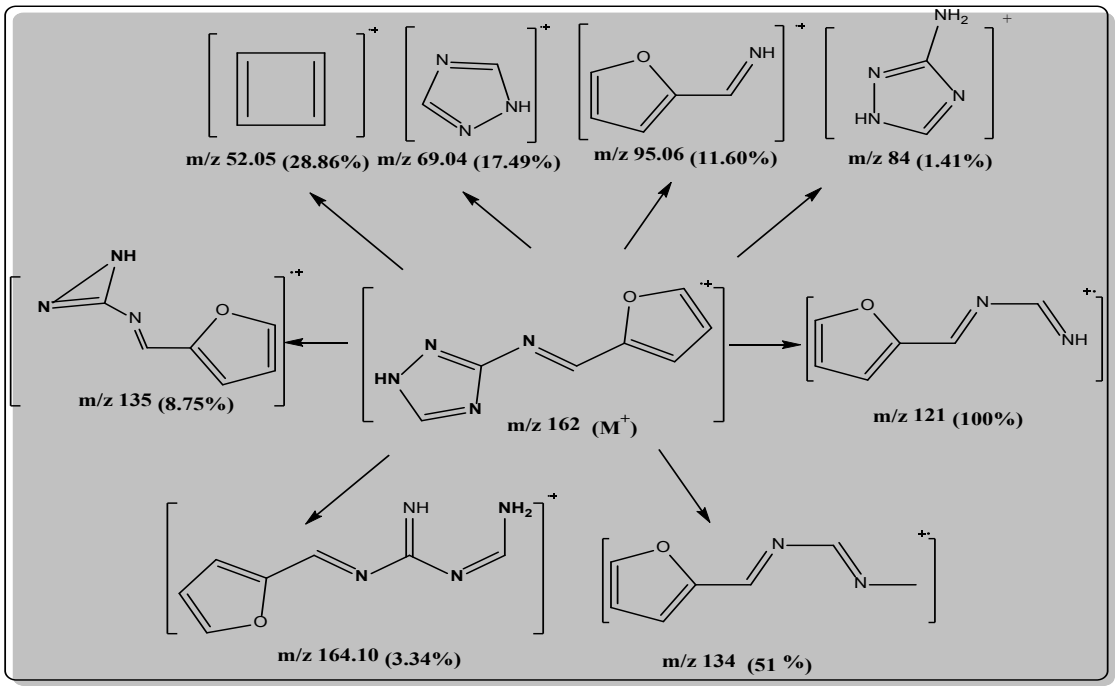

Scheme 3. Proposed mass fragmentation pattern of the ligand (FTA).

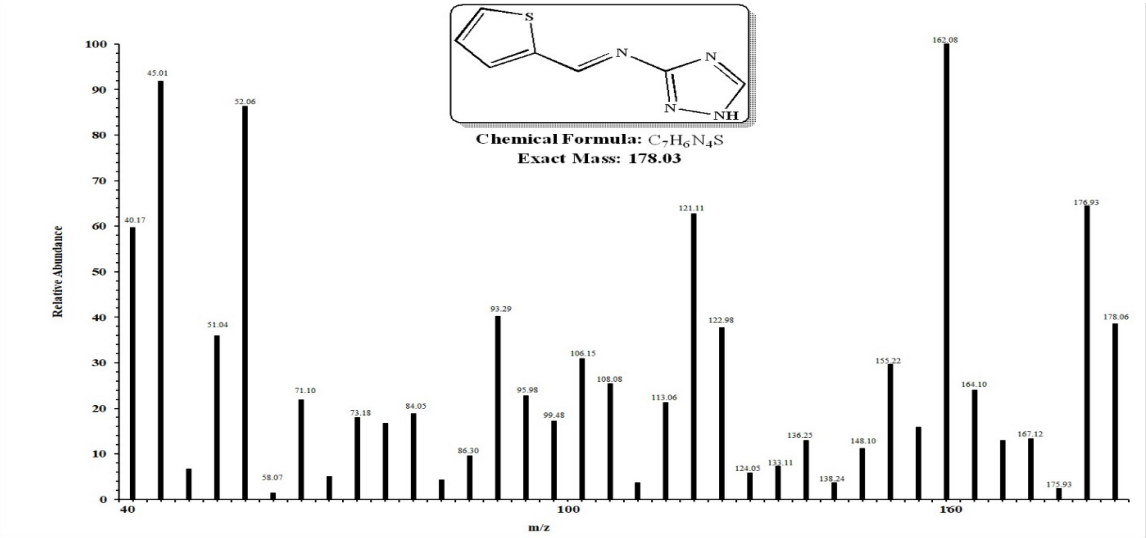

Fig. 2. Mass spectra of (TTA).

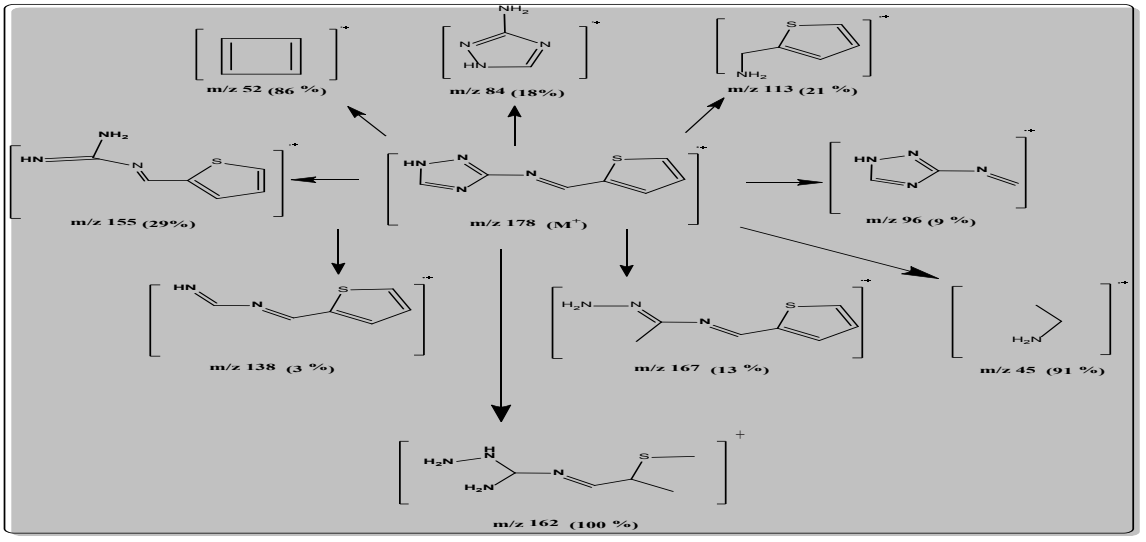

Scheme 4. Proposed mass fragmentation pattern of the ligand (TTA).

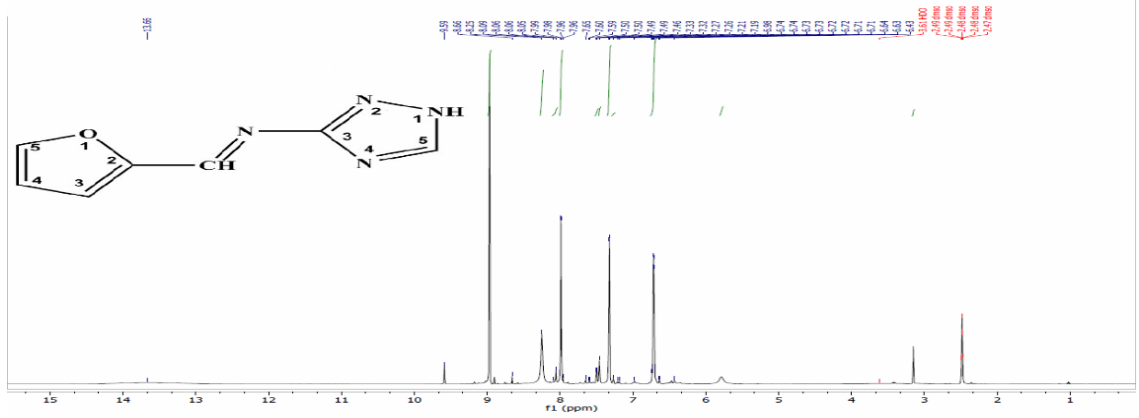

Fig. 3. [1]HNMR spectra of the (FTA) in DMSO d6 + D2O.

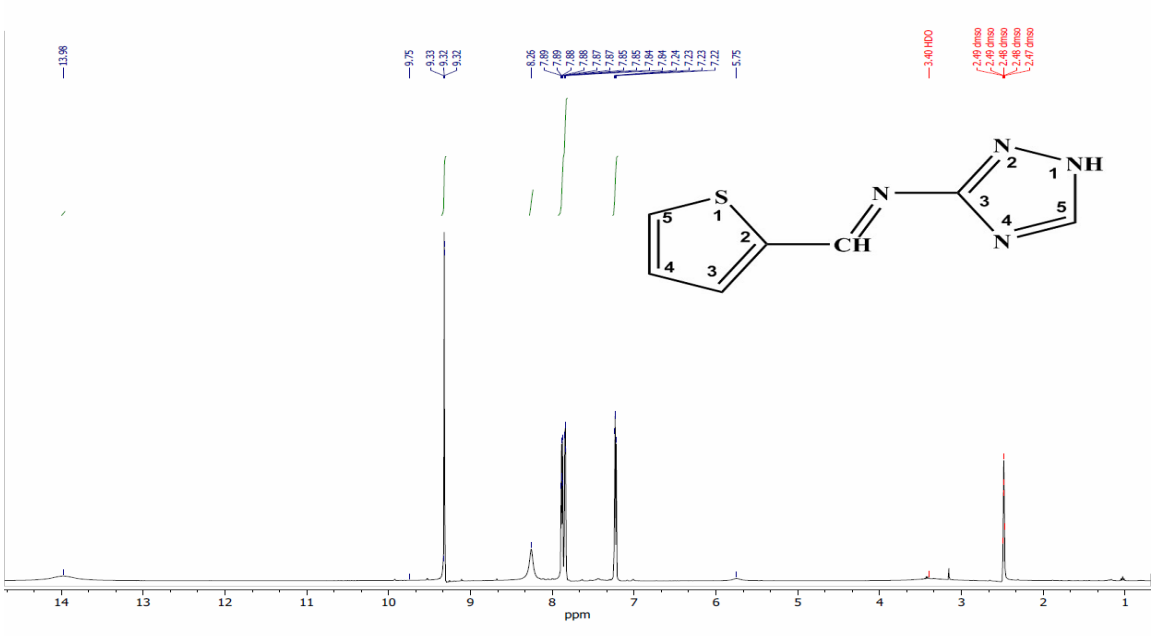

Fig. 4. [1]HNMR spectra of the (TTA) in DMSO d6 + D2O.

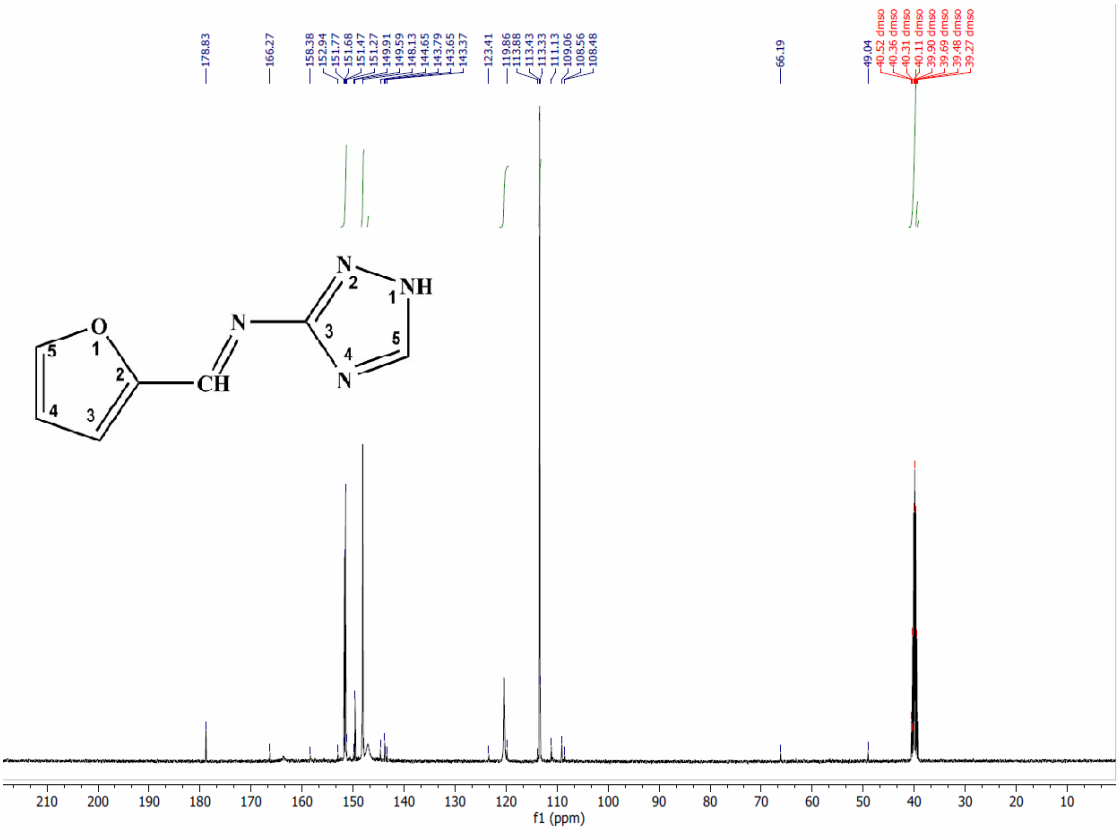

Fig. 5. [13]C NMR spectra of the (FTA) in DMSO d6.

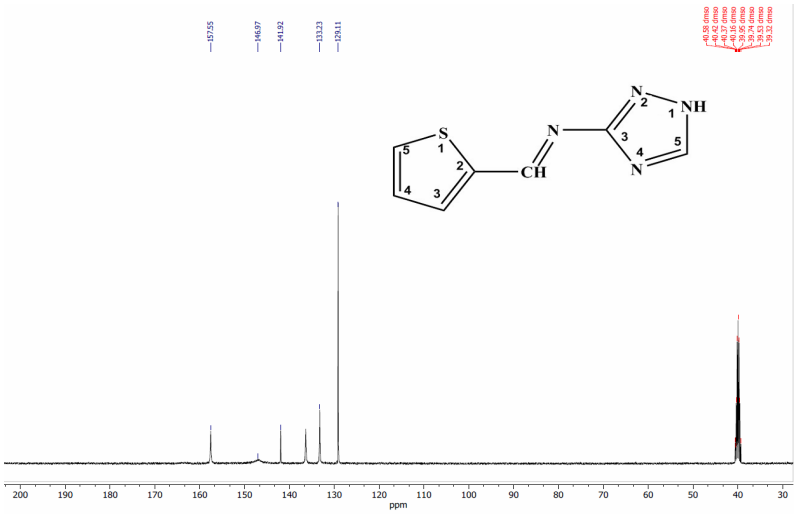

Fig. 6. ^{13}C NMR spectra of the- (TTA) in DMSO d6.

FTA showed peaks at δ = 113.325 ppm (C4 furan), 120.402 ppm (C3 furan), 144.652 ppm (C5 furan), 147.115 ppm (C, azomethine), 147.938 ppm (C5 triazole), 151.241 ppm (C2 furan), 158.385 ppm (C3 triazole), 165.47 ppm (C azomethine). The ^{13}CNMR (DMSO) spectra of the synthesized (TTA) showed peaks at δ = 157.55 ppm (C3 triazole), 146.97 ppm (CH azomethine), 141.92 ppm (C2 thiophene), 136.36 ppm (C3 thiophene), 133.23 ppm (C4 thiophene), 129.11 ppm (C5 thiophene).

Electron spin resonance Spectrum (ESR)

The spectra of the complexes exhibit a single anisotropic broad signal with hyperstructure indicating the contribution of free acetate ligand with complex formation. The ESR spectra of the Cu complexes of FTA and TTA showed broad signals with two "g" values (g\\, g⊥) (Fig. 7). For all complexes the value of g\\ < g⊥ < 2.3, characteristic of complexes with $^2B_1(d_{x^2-y^2})$ orbital ground state. The average g values were calculated according to the equation g_{av} = 1/3[g\\ +2g⊥] and it was equal to 2.14 and 2.04 for cupper complexes of FTA and TTA respectively.

Thermal analysis (TG)

Thermal analysis of Ni and Cu complexes of FTA.

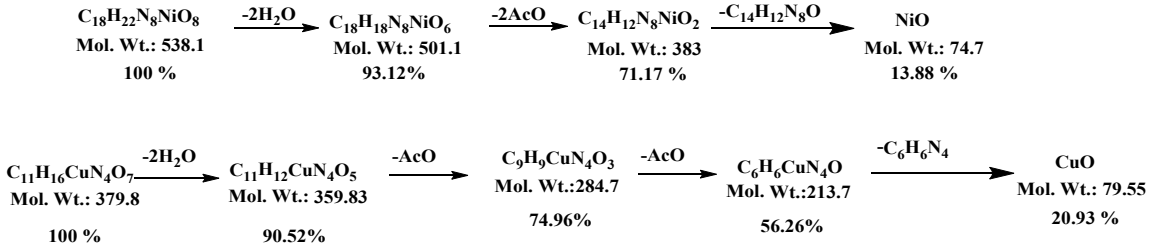

Scheme 5. Thermal decomposition scheme of Ni and Cu complexes of FTA.

Thermal analysis of Co and Zn complexes of TTA:

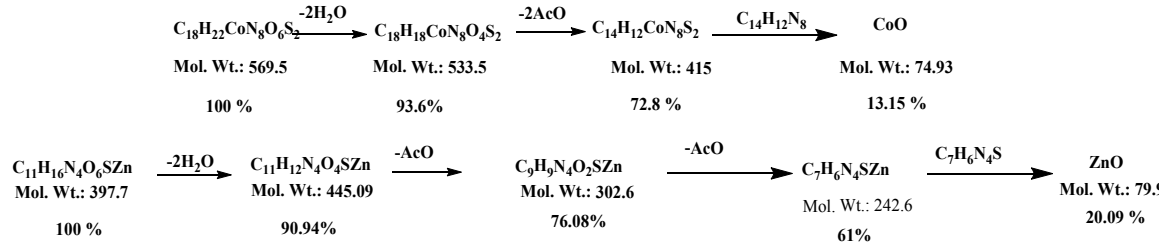

Scheme 6. Thermal decomposition scheme of Co and Zn complexes of TTA.

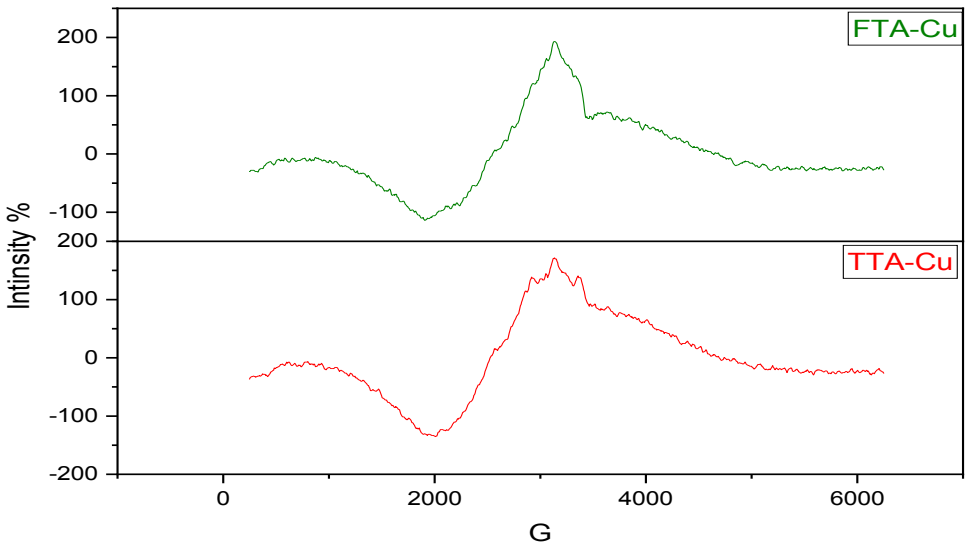

Fig. 7. ESR spectra of the Cu complexes of FTA and TTA ligands.

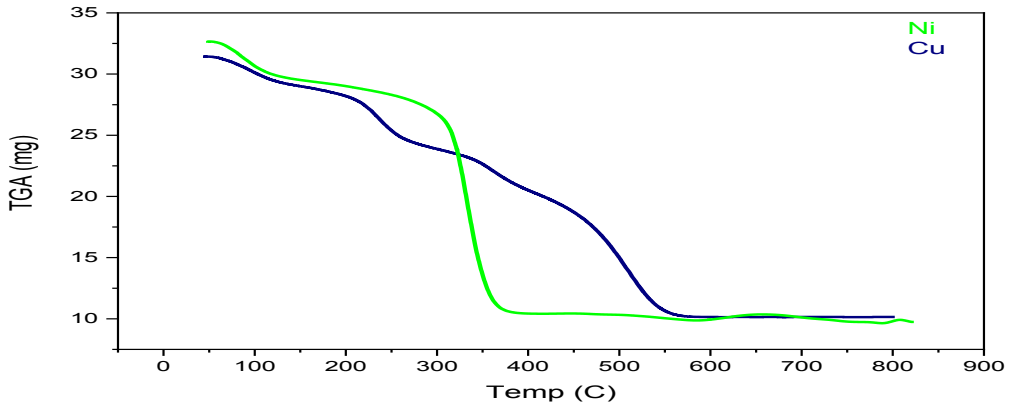

Fig. 8. Thermal analysis of FTA complexes.

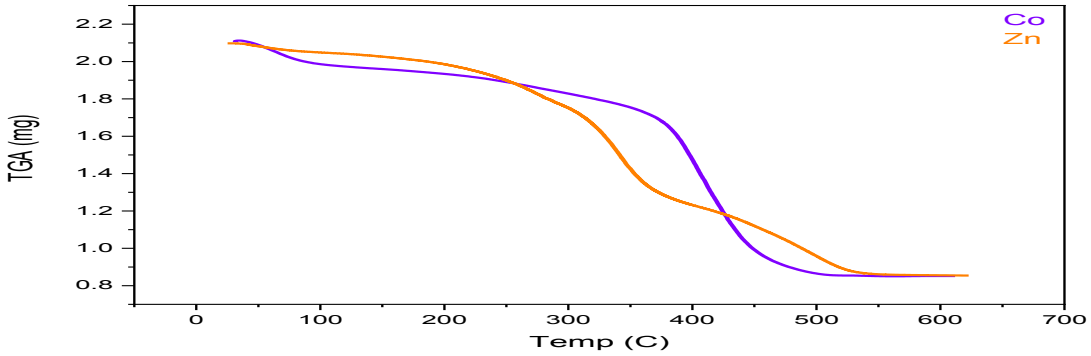

Fig. 9. Thermal analysis of TTA complexes.

TABLE 4. Thermo-gravimetric data of the thermal decomposition of Co(II), Ni(II), Cu(II) and Zn (II) complexes of the prepared ligands.

Ligand	Compd. No.	Molecular Formula	Molecular Weight	Steps	Δ T °C		mass %		Assignment
					T_i	T_f	Calc.	Found	
FTA	Cu	$C_{11}H_{16}CuN_4O_7$	379.8	1st	50	120	10.55	9.47	$2H_2O$
				2nd	160	300	16.19	15.53	AcO
				3rd	310	424	14.8	15.53	AcO
				4th	430	700	34.48	35.3	$C_6H_6N_4$
					Residue		21.98	20.93	CuO
	Ni	$C_{18}H_{22}N_8NiO_8$	538.1	1st	40	120	6.14	6.69	2H2O
				2nd	170	330	20.42	21.92	AcO
				3rd	365	409	13.19	57.29	$C_{14}H_{12}N_8O$
					Residue			13.88	NiO
TTA	Co	$C_{18}H_{22}CoN_8O_6S_2$	569.5	1st	30	120	6.67	6.36	$2H_2O$
				2nd	230	337	22.9	22.54	AcO
				3rd	379	444	56.12	59.78	$C_{14}H_{14}N_4$
					Residue		14.2	13.15	CoO
	Zn	$C_{11}H_{16}N_4O_6SZn$	397.7	1st	60	104	8.92	9.05	$2H_2O$
				2nd	277	371	13.99	14.83	AcO
				3rd	405	475	14.1	14.83	AcO
				4th	558	678	53.8	55.99	$C_7H_6N_4S$
					Residue		**19.8**	**20.09**	ZnO

Thermo-kinetic parameters:

Kinetic parameters of different stages were summarized in Table 5, together with the radii of metal ions. The results showed that the values obtained by various methods are comparable and were in harmony with each other. The kinetic and thermodynamic parameters were determined by non-isothermal methods.

From the results listed in Table 5, we get conclusions as follows:

1- The reactions are endothermic [40] and most of these reactions are slow and the reactants are less stable than products [41]

2- The rate of removal of the subsequent ligand will be lower than that of the precedent ligand and the reactions are non-spontaneous due to increasing the values of ΔG subsequently

TABLE 5. Thermodynamic data of the thermal decomposition of Co(II), Ni(II) and Cu(II) complexes of FTA and TTA.

Comp.	Steps	Coats Redfern						Horowitz-Metzger					
		R^2	Ea KJ mol^{-1}	A S^{-1}	ΔS* mol^{-1} K^{-1}	ΔH* KJ mol^{-1}	ΔG* KJ mol^{-1}	R^2	Ea KJ mol^{-1}	A S^{-1}	ΔS* mol^{-1} K^{-1}	ΔH* KJ mol^{-1}	ΔG* KJ mol^{-1}
Cu	1st	0.96	73194	5.42×10^{9}	-60	70216	91728	0.96	31966	1.38×10^{4}	-167	28990	88840
	2nd	0.99	34489	5.99×10^{16}	-204	30246	134412	0.99	21624	1.64×10^{1}	-256	17384	148051
	3rd	0.98	55183	1.18×10^{5}	-152	50998	127552	0.98	21035	1.53×10^{1}	-226	16853	130845
	4th	0.92	290288	6.06×10^{11}	-27	283316	306732	0.9	116769	3.80×10^{6}	-127	109802	216700
Ni	1st	0.94	57	4.36×10^{7}	-100	543	92586	0.93	36	2.68×10^{4}	-162	32856	94487
	2nd	0.99	34489	5.99×10^{16}	-262	30246	163929	0.99	21624	1.64×10^{1}	-253	17384	146470
	3rd	0.98	332634	2.63×10^{18}	100	327517	265529	0.98	566021	2.15×10^{48}	674	560908	146128
Co	1st	0.90	49818	3.37×10^{6}	-121	46881	89728	0.90	20719	2.33×10^{2}	-201	17785	88750
	2nd	0.99	34298	5.96×10^{16}	-262	30054	163779	0.99	21624.7	1.64×10^{1}	-253	17384	146468
	3rd	0.98	332634	2.35×10^{18}	100	327517	265529	0.98	566021	2.15×10^{48}	674	560908	146128
Zn	1st	0.93	60165	5.36×10^{7}	-98	57170	92640	0.92	28014	3.02×10^{3}	-179	25021	89782
	2nd	0.98	55950	1.20×10^{15}	-239	51349	183940	0.99	33052	1.72×10^{2}	-231	28454	156559
	3rd	0.99	454114	1.73×10^{39}	500	449197	153323	0.99	203274	6.48×10^{17}	90	198360	144933
	4th	0.99	167850	2.32×10^{11}	-34	161942	186485	0.99	75439	6.39×10^{4}	-160	69536	183248

Corrosion evaluation of the prepared Schiff base ligand by Weight loss measurements

Concentration and temperature effect

Weight loss method was applied to study the rate of corrosion of C-steel in the existence and disappearance of several concentration ranges of inhibitors FTA, and TTA at three different temperatures (Table 6). The corrosion rate value was calculated from the following equation:

$$K = \Delta W / At \quad (4)$$

where (k) is the corrosion rate (mg cm^{-2} h^{-1}), (ΔW) is the loss of weight after corrosion (mg), (A) is the total area of the coupon (cm^2), and t is the corrosion time (h) respectively.

The surface coverage degree (θ) and the efficiency of inhibition n_w%, were estimated from the following equations [42]:

$$\theta = \frac{K_0 - K}{K_0} \quad (5)$$

$$n\% = \frac{K_0 - K}{K_0} \times 100 \quad (6)$$

where k_o and k are the corrosion rate values without and with the addition of the inhibitor, respectively. From Table 6, it's obvious that the inhibition efficiency percentage (n_w%) increases when the inhibitor concentration also increases which corresponds to the increase in the mass and charge transfer to the C-steel surface causing the inhibitor molecules to be adsorbed on the metal surface that is positively influencing the reduction of metal dissolution. Moreover, an increasing in surface area (θ) coverage took place by increasing inhibitor concentration. It was also indicated that variation of temperature affects the inhibition percentage at an in the direct way which means that, inhibition efficiency decreases with the increase in temperature. Because at high temperatures, the hydrogen development increases on the metal surface cussing to the desorption of the adsorbed inhibitor film from the metal surface [43]. So that, the prepared compounds were suggested to be of good inhibition efficiency as inhibitors for C-steel dissolution in 1.0 M HCl solution, and the order of the inhibition efficiencies of the two greenly synthesized Schiff base inhibitors increases in the following order: FTA < TTA.

Adsorption isotherm

According to corrosion studies, it is significant to recognize the relationship between the metal surface and the inhibitor molecules. This relationship comes to light when an adsorption process occurs through two different pathways. Generally, adsorption of an inhibitor may be categorized as physical adsorption and chemisorption. The main factors influencing the adsorption type are the metal electronic configuration, electrolyte type and the chemical structure of the inhibitor. Furthermore, adsorption process takes place when water molecules ($H_2O_{(ads)}$) that were already adsorbed on the substrate surface are displaced by the inhibitor

TABLE 6. Weight loss data for steel 1.0 M HCl without and with different concentrations of the Schiff bases at various temperatures.

Inhibitor name	Conc. (M)	30 °C			40 °C			50 °C		
		k	θ	η_w	k	θ	η_w	k	θ	η_w
		(mg.cm^{-2}.h^{-1})		(%)	(mg.cm^{-2}.h^{-1})		(%)	(mg.cm^{-2}.h^{-1})		(%)
blank	0×10^{-4}	26.40 x 10^{-2}	-----	-----	24.57 x 10^{-2}	-----	------	102.42 x 10^{-2}	------	------
FTA	0.5×10^{-4}	8.04 x 10^{-2}	0.70	69.57	18.30 x 10^{-2}	0.26	25.53	64.44 x 10^{-2}	0.37	37.08
	0.75×10^{-4}	6.01 x 10^{-2}	0.77	77.23	15.20 x 10^{-2}	0.38	38.13	55.49 x 10^{-2}	0.46	45.82
	1×10^{-4}	5.29 x 10^{-2}	0.80	79.98	14.06 x 10^{-2}	0.43	42.78	49.79 x 10^{-2}	0.51	51.39
	5×10^{-4}	3.61 x 10^{-2}	0.86	86.34	9.40 x 10^{-2}	0.62	61.72	38.60 x 10^{-2}	0.62	62.32
	10×10^{-4}	1.99 x 10^{-2}	0.92	92.47	8.05 x 10^{-2}	0.67	67.25	19.63 x 10^{-2}	0.81	80.83
TTA	0.5×10^{-4}	7.48 x 10^{-2}	0.72	71.69	18.06 x 10^{-2}	0.27	26.50	62.31 x 10^{-2}	0.39	39.16
	0.75×10^{-4}	5.56 x 10^{-2}	0.79	78.94	14.46 x 10^{-2}	0.41	41.13	53.71 x 10^{-2}	0.48	47.55
	1×10^{-4}	4.58 x 10^{-2}	0.83	82.64	12.30 x 10^{-2}	0.50	49.95	42.85 x 10^{-2}	0.58	58.17
	5×10^{-4}	2.86 x 10^{-2}	0.89	89.18	8.77 x 10^{-2}	0.64	64.29	27.19 x 10^{-2}	0.73	73.45
	10×10^{-4}	1.79 x 10^{-2}	0.93	93.24	7.18 x 10^{-2}	0.71	70.78	19.06 x 10^{-2}	0.81	81.39

molecules ($Inh_{(sol)}$) exists in the aqueous solution as follows [44-46]:

$$Org_{(sol)} + xH_2O_{(ads)} \rightarrow Org_{(ads)} + xH_2O_{(sol)} \quad (7)$$

Where the size ratio (x) represents the number of replaced water molecules by one organic molecule.

Different adsorption isotherm equations such as Freundlich, Langmuir, Frumkin, Flory-Huggins, Frumkin, and Temkin can be applied to the data resulted from weight loss, but it was found that the data obtained from weight loss are more likely to fit with the Langmuir isotherm especially when the correlation coefficients (R^2) for, FTA and TTA are 0.9997, 0.9991 and 0.9997 respectively. The Langmuir relation is as follows [47,48]:

$$\text{Langmuir Isotherm} = C_{inh} / \theta = 1 / k_{ads} + C_{inh} \quad (8)$$

Where C_{inh} is the inhibitor concentration, K_{ads} is the equilibrium constant of the isotherm process and θ is the degree of surface coverage. By plotting C_{inh}/θ against C as shown in Fig. 10, it was clear that the slope of Langmuir adsorption isotherm for the three synthesized inhibitors, FTA and TTA at 30 °C was almost close to unity except a slight deviation took place, which may be referred to the interaction among the adsorbed inhibitor molecules with each other [49,50]. Values of the equilibrium constant (K_{ads}) for inhibitors TTA and FTA were 45.88 × 10^3 and 55.52 × 10^3 respectively, these high values indicate how strong the adsorption force between the synthesized inhibitors and the surface of the metal. It is also known that the equilibrium constant (K_{ads}) is related to the Gibbs free energy according to the equation [51]:

$$\Delta G^\circ_{ads} = - RT \ln (55.5\ K_{ads}) \quad (9)$$

Where (55.5) is the molar concentration of water in solution expressed in mole/l, *T* is the absolute temperature and *R (8.314)* is the universal gas constant. Generally, when ΔG°_{ads} values are equal to -20 or higher it may be considered as (Physical adsorption), while values of -40 or lower are of the type (chemisorption) [52]. Calculated values of the Gibbs free energy for inhibitors, TTA, and FTA were - 37.1628 and – 37.6436 KJ mol^{-1}. So it is obvious that this value shows that the adsorption processes were of chemically adsorption type on the substrate surface plus it also brings to light that an electron transfer process took place to form a coordination bond among the inhibitor molecules and the d-orbital of the iron molecules [53,54]. Enthalpy and Entropy of adsorption can be calculated as follows:

$$\ln K_{ads} = \left(\frac{\Delta H_{ads}}{RT}\right) + \text{const} \quad (10)$$

$$\Delta G = \Delta H_{ads} - T\Delta S_{ads} \quad (11)$$

Where ΔH_{ads} and K_{ads} are the adsorption heat and adsorptive equilibrium constant, respectively. Plotting ln K_{ads} against *1/T* gives straight line which slope is equal to ΔH_{ads} /R. Negative values of ΔH_{ads} are shown in Table 7 suggests that the adsorption of inhibitors is exothermic in nature. In addition, the negative values of ΔH_{ads} show that the adsorption is exothermal with an ordered phenomenon ascribed by the negative values of ΔS_{ads}. This order may more probably be clarified by the possibility of formation of the iron complex on the metal surface [55,56].

Activation parameters

The Arrhenius-type equation was applied to calculate activation energy *(E^*),* the enthalpy of activation *(ΔH^*),* and the entropy of activation *(ΔS^*)* for C-steel coupons in 1M HCl in the presence and absence of the synthesized inhibitor, FTA and TTA according to equations **(9)** as follows:

$$Log(k) = Ae^{E_a/RT} \quad (9)$$

Where A, k, T and R represents the Arrhenius constant, the corrosion rate obtained from weight loss measurement, the absolute temperature, and *R* is the universal gas constant. Figure 11 shows a graph of plotting log k against 1/T in our two investigated phases with and without several ranges of inhibitors concentrations, the graph shows a straight line with a slope of ($-E_a/2.303R$). From Table 8, it can be acknowledged that the activation energy in absence of inhibitor is lower than in their presence which implies that the corrosion rate of C-steel is reduced by forming the iron-inhibitor complex [57]. Calculations of Enthalpy and Entropy of activation were done using equation (10) as follows:

$$K = \left(\frac{RT}{Nh}\right) \exp\left(\frac{\Delta S^*}{R}\right) \exp\left(-\frac{\Delta H^*}{RT}\right) \quad (10)$$

Where *k, T, R, N, h represents,* the corrosion rate, the absolute temperature, the universal gas constant, the Avogadro's number and the Planck's constant respectively. log*(k)* was plotted against

TABLE 7. Thermodynamic parameters using Langmuir adsorption isotherm on steel surface in 1.0 M HCl containing different concentrations of the Schiff bases.

Inhibitor	Temp. (°k)	K_{ads} (KJ/mol)	ΔG_{ads} (KJ/mol)	ΔS_{ads} (J/mol .°k)	ΔH_{ads} (KJ/mol)
FTA	303	45.882	-37.16	-77.22	-60.56
	313	9.328	-33.14	-87.58	
	323	10.541	-33.45	-83.91	
TTA	303	55.528	-37.64	-59.74	-55.74
	313	10.517	-33.45	-71.22	
	323	14.402	-34.24	-66.57	

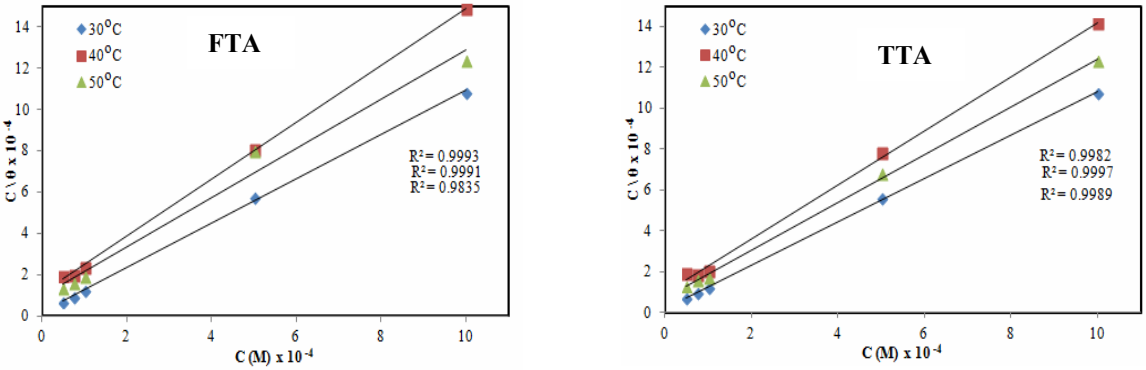

Fig. 10. Langmuir isotherm adsorption model on the carbon steel surface of Schiff base inhibitor FTA and TTA in 1.0 M HCl at different temperatures.

TABLE 8. Activation parameters values for steel in 1.0 M HCl in the absence and presence of different concentrations of the synthesized Schiff bases.

inhibitor	Conc. of inhibitor (M)	E_a (kJ mol^{-1})	ΔH* (kJ mol^{-1})	ΔS* (kJ mol^{-1} K^{-1})
blank	0×10^{-4}	54.48	78.05	153.16
FTA	0.5×10^{-4}	84.49	122.72	288.38
	0.75×10^{-4}	90.24	131.50	314.02
	1×10^{-4}	91.10	133.12	318.00
	5×10^{-4}	96.21	141.37	340.37
	10×10^{-4}	93.36	139.71	329.57
TTA	0.5×10^{-4}	86.09	125.14	295.64
	0.75×10^{-4}	92.10	134.29	322.32
	1×10^{-4}	90.80	133.24	316.73
	5×10^{-4}	91.64	136.07	320.93
	10×10^{-4}	96.49	144.30	343.26

$1/T$, a straight line with slope equal to $\Delta H^*/2.303R$ and an intercept equal to log $(R/Nh) + \Delta S^*/2.303R$ *were* obtained as presented in Fig. 11.

It is obvious that values of ΔS^* are greater when the inhibitor exists in the acidic solution than in uninhibited solution which is generally explicated as an increase in disorder as the reactants are transformed to the activated complexes. Thus, it suggested that a displacement process of water molecules over adsorption of inhibitors on the C-steel surface took place.

Biological activity.

Antimicrobial activity

To contribute to the field of bioinorganic chemistry, the synthesized ligand and its Zn(II) complex were tested against bacterial and fungal strains by disc diffusion method (*cf* experimental part). The results were compared with those of the standard drugs (Gentamicin for Gram-positive bacteria and Gram-negative bacteria and Ketoconazole for fungal strains) and calculated the diameter of inhibition zone for each by mm. The antimicrobial results evidently showed that the triazole derivatives and its complexes possess a broad spectrum of activity against the tested organisms.

Antimicrobial activity of Ligands and their Zn(II) complex

The antimicrobial activity of ligands and their Zn(II) complexes against the bacterial and fungal strains were tested and evaluated. Table 9 shows the antimicrobial activity of ligand against the tested bacterial and fungal strains. Our results showed no inhibition effect on the growth of the bacterial and fungal strains by the ligand excepted the effect on the growth of Bacillus subtillus RCMB 015 (1) NRRL B-543, Aspergillus fumigatus (RCMB 002008) and Candida albicans RCMB 005003 (1) ATCC 10231 with inhibition zones 9 mm, 17 mm and 15 mm, respectively. While the Zn (II) complex exhibited good antimicrobial activity against both bacteria (Gram-negative & Gram-positive bacteria) and fungal strains. It showed higher antibacterial activity against Bacillus subtillus RCMB 015 (1) NRRL B-543, Staphylococcus aureus (RCMB010010) and Escherichia Coli (RCMB 010052) ATCC 25955 with inhibition zone 15 mm, 13 mm and 14 mm respectively, while appearance moderated to weak activity against Aspergillus fumigatus (RCMB 002008) and Candida albicans RCMB 005003 (1) ATCC 10231 with inhibition zone 16 and 14 mm, respectively. Hence the antimicrobial activity after complexation with Zn(II) is enhanced as compared to that of the free ligand.

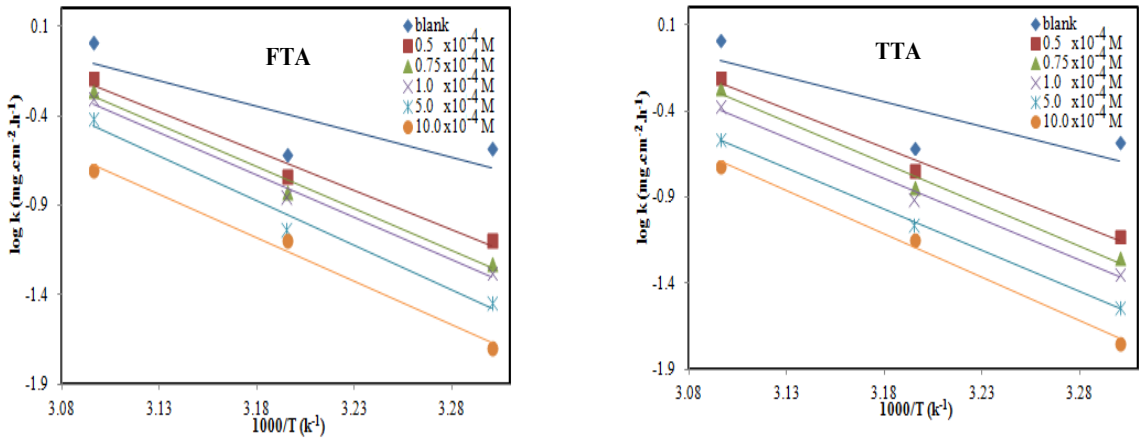

Fig. 11. Arrhenius plots (log k vs. 1/T) for steel dissolution in the absence and the presence of different concentrations of FTA and TTA in 1.0 M HCl solution.

TABLE 9. The antimicrobial activity of the ligands and their Zn(II) complex.

Comp.	Recorded zone diameter (mm) for each test microorganism					
	BACTRIA				FUNGI	
	Gram-positive		Gram-negative			
	Bacillus subtillus RCMB 015 (1) NRRL B-543	Staphylococcus aureus (RCMB010010)	Escherichia Coli (RCMB 010052) ATCC 25955	Salmonella typhimurium RCMB 006 (1) ATCC 14028	Aspergillus fumigatus (RCMB 002008)	Candida albicans RCMB 005003 (1) ATCC 10231
FTA	10	NA	NA	NA	NA	NA
Zn	12	11	9	10	NA	NA
TTA	NA	NA	NA	NA	NA	NA
Zn	11	10	14	16	NA	11
St.	26	24	30	17	17	20

Conclusions

1. Using the microwave method assures the principals of green chemistry.
2. The structure of the prepared compounds was spectroscopically illustrated by FT-IR, UV-Vis, NMR, Mass, and elemental analysis.
3. The newly synthesized Schiff bases ligand act as a bidentate and tridentate ligand, which coordinated through the azomethine-N, oxygen-O, sulfur-S and triazole ring to the metal ions; Co (II), Ni (II), Cu (II) and Zn (II).
4. The thermal dehydration and decomposition of Ni (II), Co (II), Cu (II) and Zn (II) complex show elimination of water, acetate then organic content and MO remained as a residue.
5. The antimicrobial activity of the Schiff base ligands and their Zn (II) complexes against the bacterial and fungal strains showed that the activity of the ligand after complexation with Zn (II) is enhanced as compared to that of the free ligand.
6. Obtained results from weight loss measurements approved that the adsorption of the prepared inhibitors FTA and TTA at the metal/acid solution interface occurs in a good and efficient manner.
7. The presence of heteroatoms and iminic groups form a strong protective film as it increases the adsorption of compounds on C-steel surface which make these interactions are more than electrostatic one.

References

1. Ehsan. S, Ishfaq. A, Khan. B, Saghir. T, Ghafoor. S. Conventional & Microwave-Assisted Synthesis and Antimicrobial Evaluation of Pyrimidine Azo Compounds. *International J. of Science and Research,* **3**(12), 368-373 (2012).
2. Ahmed Younis, Ali, M. Hassan, Mohamed, F. Mady, El-Haddad A. F., Yassin, F. A., Mahmoud Fayad. Microwave-Assisted One-Pot Synthesis of Novel Polyarylpyrrole Derivatives of Expected Anticancer Activity. *Der Pharma Chemica,* **9**(3), 33-44 (2017).
3. Ahmed Younis, Ali, M. Hassan, Mohamed, F. Mady, El-Haddad A. F., Mahmoud Fayad. Utilization of Microwave Irradiation and Conventional Methods on Synthesis of Novel Pyridine Derivatives of Expected Anticancer Activity *Journal of Chemical and Pharmaceutical Research*, **8**(9), 193-202 (2016).
4. El-Kateb, A.A, Abd El-Rahman, N.M.; Saleh, T.S.; Ali, M. Hassan; El-Dosoky, A.Y. and Ghada E. A. Awad Microwave assisted 1,3-Dipolar Cycloaddition Reactions of Some Nitrilimines and Nitrile Oxide to E-1-(4-(1-(4-aminophenyl) ethylideneamino)phenyl)-3-(dimethylamino) prop-2-ene-1-one under solventless conditions. *Journal of Applied Sciences Research*, **8**(7), 3393-3405 (2012).
5. Rao, K. J.; Vaidhyanathan, B.; Ganguli,M.;

Ramakrishnan, P. A.; Microwave-Assisted Solid-State Synthesis of Oxide Ion Conducting Stabilized Bismuth Vanadate Phases. *Chem. Mater.* **11**, 882 (1998).

6. Kappe. C. O, Dallinger. D, Murphree. S. S. *Practical Microwave Synthesis for Organic Chemists: Strategies, Instruments, and Protocols* Wiley-VCH, Weinheim, Germany (2009).

7. Kappe. C. O. Controlled microwave heating in modern organic synthesis. *Angewandte Chemie International Edition,* **43**(46), 6250-6284 (2004).

8. Shi. S, Hwang J. Y. Microwave-assisted wet chemical synthesis: advantages, significance, and steps to industrialization. *Journal of Minerals and Materials Characterization and Engineering,* **2**(02), 101 (2003).

9. a) Kubrakova. I.V. Effect of microwave radiation on physicochemical processes in solutions and heterogeneous systems: applications in analytical chemistry. *Journal of Analytical Chemistry,* **55**(12), 1113-1122 (2000).

   b) Banach,Ł.; Guńka, P.A.; Zachara, J.; Buchowicz, W. Half-sandwich Ni(II) complexes [Ni(Cp)(X)(NHC)]: From an underestimated discovery to a new chapter in organonickel chemistry. *Coordination Chemistry Reviews,* **389**, 19-58, (2019).

10. Nassar, A. M., Hassan, A. M., Ibraheem, N. M., & Hekal, B. H. Synthesis and Comparative Studies of Cyclopalladated Complexes With Ortho C–H Activation of Aromatic Rings Bearing Electron Donating and Electron Withdrawing Groups. *Synthesis and Reactivity in Inorganic, Metal-Organic, and Nano-Metal Chemistry*, **45**(6), 813-820 (2015).

11. Ali, A. M., Ahmed, A. H., Mohamed, T. A., & Mohamed, B. H. Geometrical studies on iron (III), palladium (II) and platinum (IV) complexes of bis-Schiff bases derived from aromatic diammine and corrosion inhibitions of ligands. *Journal of Applied Sciences Research*, **3**(2), 109-118 (2007).

12. Ali M. Ali, Ayman H. Ahmed, Tarek A. Mohamed and Bassem H. Mohamed, Chelates and corrosion inhibition of newly synthesized Schiff bases derived from o-tolidine. *Transition Metal Chemistry*, **11243,** 184-188 (2007).

13. Ali M. Hassan, Amr M. Nassar, Bassem H. Heakal, N. M. Abdelrahman."Complexation behavior of newly synthesized Schiff base N-(4-methoxyphenyl-4\-cyanobenzilidene) as corrosion inhibition". *Al-Azhar Bull. Sci*. **22** (2), 25-36 (Dec.: 2011).

14. Monshi, M. A. S., AbdelSalam, N. M., & Salamah, A. A. Complexes of a Schiff base formed by the condensation of S-benzyl dithiocarbazate and benzoyl acetone. *Journal of the Chemical Society of Pakistan*, **18**(3), 214-219 (1996).

15. Raman, N.; Kulandaisamy, A.; Thangaraja, C.;Manisankar, P.;Viswanathan, S. Vedhi, C. Synthesis, structural characterisation and electrochemical and antibacterial studies of Schiff base copper complexes. *Transition Metal Chemistry*, **29** (2), 129–135 (2004).

16. Das, M., & Livingstone, S. E. Metal chelates of dithiocarbazic acid and its derivatives. IX. Metal chelates of ten new Schiff bases derived from S-methyldithiocarbazate. *Inorganica Chimica Acta*, **19**, 5-10 (1976).

17. Jarrahpour, A.; Khalili, D.; Clercq, E.; Salmi, C.; Brunel, J. M.; Synthesis, Antibacterial, Antifungal and Antiviral Activity Evaluation of Some New bis-Schiff Bases of Isatin and Their Derivatives, *Molecules* **12**(8), 1720-1730 (2007).

18. Jayabalakrishnan, C.; Natarajan, K.; Ruthenium(II) carbonyl complexes with tridentate Schiff bases and their antibacterial activity *Transition Metal Chemistry,* **27** (1), 75-79 (2002).

19. Singh, H.L. and A.K. Varshney, Synthesis and characterization of coordination compounds of organotin(IV) with nitrogen and sulfur donor ligands. *Appl. Organometal Chem*. **15**(9), 762-768 (2001).

20. Ali, M. A., Mirza, A. H., Butcher, R. J., & Rahman, M. Nickel (II), copper (II), palladium (II) and platinum (II) complexes of bidentate SN ligands derived from S-alkyldithiocarbazates and the X-ray crystal structures of the [Ni (tasbz) 2] and [Cu (tasbz) 2]· CHCl3 complexes. *Transition Metal Chemistry*, **25**(4), 430-436 (2000).

21. Balabin. R. M. Tautomeric equilibrium and hydrogen shifts in tetrazole and triazoles: Focal-point analysis and ab initio limit. *The Journal of Chemical Physics*, **131**(15), 154-307 (2009).

22. Gopi. D, Govindaraju. K. M, Kavitha. L. Investigation of triazole derived Schiff bases as corrosion inhibitors for mild steel in hydrochloric acid medium. *Journal of Applied Electrochemistry*, **40**(7), 1349-1356 (2010).

23. Swathi. N. P, Alva. V. D, Samshuddin. S. A Review on 1,2,4-Triazole Derivatives as Corrosion Inhibitors. *Journal of Bio- and Tribo-Corrosion*, **3**(4), 42 (2017).

24. Frolova. L. V, Kuznetsov. Y. I. Inhibition of carbon steels from hydrogen-sulfide corrosion with triazoles. *Protection of Metals and Physical Chemistry of Surfaces*, **45**(7), 796 (2009).

25. Bentiss. F, Lagrenee. M, Traisnel. M, Mernari. B, Elattari. H. 3,5-bis(n-Hydroxyphenyl)-4-amino-1,2,4-triazoles and 3,5-bis(n-aminophenyl)-4-amino-1,2,4-triazoles: a new class of corrosion inhibitors for mild steel in 1m HCl medium. *Journal of Applied Electrochemistry*, **29**(9), 1073-1078 (1999).

26. ElKateb, A. A., Saleh, T. S., Ali, M. H., Elhaddad, A. S., & El-Dosoky, A. Y. Microwave mediated facile synthesis of some novel pyrazole, pyrimidine, pyrazolo [1, 5-a] pyrimidine, triazolo [1, 5-a] pyrimidine and pyrimido [1, 2-a] benzimidazole derivatives under solvent less condition. *Nat Sci*, **10**(11), 77-86 (2012).

27. Ahmed Younis, Usama Fathy, A. Atef El-kateb and Hanem M. Awad Ultrasonic assisted synthesis of novel anticancer chalcones using water as green solvent. *Der Pharma Chemica*, 8**(**17), 129-136 (2016).

28. Fathy, U., A. Younis, and H. Awad, Ultrasonic assisted synthesis, anticancer and antioxidant activity of some novel pyrazolo[3,4-b] pyridine derivatives. *Journal of Chemical and Pharmaceutical Research,* **7**(9), 4-12 (2015).

29. Furniss. B. S. *Vogel's Textbook of Practical Organic Chemistry*: Pearson Education India (1989).

30. Coats. A. W, Redfern. J. P. Kinetic parameters from thermogravimetric data. *Nature*, **201**(4914), 68-69 (1964).

31. Horowitz. H. H, Metzger. G. A new analysis of thermogravimetric traces. *Analytical Chemistry,* **35**(10), 1464-1468 (1963).

32. Cooper. R, Kavanagh. F. *Analytical Microbiology,* **1**(2), (1972).

33. Hassan. A. M, Heakal. B. H, Awad. B, Khamis. H, Abd El-Naeem. G, Abd-Elsatar. M. Green and efficient synthesis, characterization, antimicrobial and colon carcinoma (HCT 116) of transition metals (Mn(II)m Co(II), Ni(II) and Cu(II)) complexes with (1,2,4-triazol-3-ylimino)methyl)-6-methoxyphenol. *Al-Azhar Bulletin of Science*, **9**, 157-176 (2017).

34. Finney. D. J. *Probit Analysis:* 3d Ed: Cambridge University Press, (1971).

35. El-Wahab. H. A, El-Fattah. M. A, Ahmed. A. H, Elhenawy. A. A, Alian. N. Synthesis and characterization of some arylhydrazone ligand and its metal complexes and their potential application as flame retardant and antimicrobial additives in polyurethane for surface coating. *Journal of Organometallic Chemistry*, **79**, 99-106 (2015).

36. McCollum. D. G, Bosnich. B. Cooperative bimetallic reactivity. *Inorganica Chimica Acta*, **270**(1), 13-9 (1998).

37. Yoe. J. H, Jones. A. L. Colorimetric determination of iron with disodium-1, 2-dihydroxybenzene-3, 5-disulfonate. *Industrial & Engineering Chemistry Analytical Edition*, **16**(2), 111-115 (1944).

38. Chohan. Z. H, Sumrra. S. H, Youssoufi. M. H, Hadda. T. B. Design and synthesis of triazole Schiff bases and their oxovanadium (IV) complexes as antimicrobial agents. *Journal of Coordination Chemistry*, **63**(22), 3981-3998 (2010).

39. Prashanthi. Y, Raj. S. Synthesis and characterization of transition metal complexes with N, O; N, N and S, N-donor Schiff base ligands. *Journal of Scientific Research*, **2**(1), 114-126 (2010).

40. El-Ayaan. U, Kenawy. I, El-Reash. Y. A. Synthesis, thermal and spectral studies of first-row transition metal complexes with Girard P reagent-based ligand. *Spectrochimica Acta Part A: Molecular and Biomolecular Spectroscopy,* **68**(2), 211-219 (2007).

41. Frost. A. A, Pearson. R. G, New York. *Kinetics and Mechanism.* John Wiley and Sons. Inc., New York, (1961).

42. Bedair. M. A, Soliman. S. A, Metwally. M. S. Synthesis and characterization of some nonionic surfactants as corrosion inhibitors for steel in 1.0 M HCl (Experimental and computational study). *Journal of Industrial and Engineering Chemistry*, **41**, 10-22 (2016).

43. Dohare. P, Chauhan. D. S, Sorour. A. A, Quraishi. M. A. DFT and experimental studies on the inhibition potentials of expired Tramadol drug on mild steel corrosion in hydrochloric acid. *Materials Discovery*, **9**, 30-41 (2017).

44. Ji. Y, Xu. B, Gong. W, Zhang. X, Jin. X, Ning. W,

Meng. Y, Yang. W, Chen. Y. Corrosion inhibition of a new Schiff base derivative with two pyridine rings on Q235 mild steel in 1.0 M HCl. *Journal of the Taiwan Institute of Chemical Engineers*, **66**, 01-12 (2016).

45. Ammal. P. R, Prajila. M, Joseph. A. Effect of substitution and temperature on the corrosion inhibition properties of benzimidazole bearing 1, 3, 4-oxadiazoles for mild steel in sulphuric acid: Physicochemical and theoretical studies. *Journal of Environmental Chemical Engineering,* **6**(1), 1072-1085 (2018).

46. Nwanonenyi. S. C, Obasi. H. C, Oguzie. E. E, Chukwujike. I. C, Anyiam. C. K. Inhibition and Adsorption of Polyvinyl Acetate (PVAc) on the Corrosion of Aluminium in Sulphuric and Hydrochloric Acid Environment. *Journal of Bio- and Tribo-Corrosion*, **3**(4), 53 (2017).

47. Elemike. E. E, Nwankwo. H. U, Onwudiwe. D. C, Hosten. E. C. Synthesis, crystal structures, quantum chemical studies and corrosion inhibition potentials of 4-(((4-ethylphenyl)imino)methyl) phenol and (E)-4-((naphthalen-2-ylimino) methyl) phenol Schiff bases. *Journal of Molecular Structure*, **1147**, 252-265 (2017).

48. Musa. A. Y, Jalgham. R. T. T, Mohamad. A. B. Molecular dynamic and quantum chemical calculations for phthalazine derivatives as corrosion inhibitors of mild steel in 1M HCl. *Corrosion Science*, **56**, 176-183 (2012).

49. Bedair. M. A, El-Sabbah. M. M. B, Fouda. A. S, Elaryian. H. M. Synthesis, electrochemical and quantum chemical studies of some prepared surfactants based on azodye and Schiff base as corrosion inhibitors for steel in acid medium. *Corrosion Science*, **128**, 54-72 (2017).

50. Tao. Z, Zhang. S, Li. W, Hou. B. Corrosion inhibition of mild steel in acidic solution by some oxo-triazole derivatives. *Corrosion Science*, **51**(11), 2588-2595 (2009).

51. John. S. A. M, Ali. K. M, Joseph. A. Electrochemical, surface analytical and quantum chemical studies on Schiff bases of 4-amino-4H-1, 2, 4-triazole-3,5-dimethanol (ATD) in corrosion protection of aluminium in 1N HNO3. *Bulletin of Materials Science*, **34**(6), 1245-1256 (2011).

52. Sobhi. M, El-sayed. R, Abdallah. M. The Effect of Non Ionic Surfactants Containing Triazole, Thiadiazole and Oxadiazole as Inhibitors of the Corrosion of Carbon Steel in 1M Hydrochloric Acid. *Journal of Surfactants and Detergents*, **16**(6), 937-946 (2013).

53. Abd El-Lateef. H. M. Experimental and computational investigation on the corrosion inhibition characteristics of mild steel by some novel synthesized imines in hydrochloric acid solutions. *Corrosion Science*, **92**, 104-117 (2015).

54. Abd El-Lateef. H. M, Abo-Riya. M. A, Tantawy. A. H. Empirical and quantum chemical studies on the corrosion inhibition performance of some novel synthesized cationic gemini surfactants on carbon steel pipelines in acid pickling processes. *Corrosion Science*, **108**, 94-110 (2016).

55. Haque. J, Ansari. K. R, Srivastav. V, Quraishi. M. A, Obot. I. B. Pyrimidine derivatives as novel acidizing corrosion inhibitors for N80 steel useful for petroleum industry: A combined experimental and theoretical approach. *Journal of Industrial and Engineering Chemistry*, **49**, 176-188 (2017).

56. Herrag. L, Chetouani. A, Elkadiri. S, Hammouti. B, Aouniti. A. Pyrazole Derivatives as Corrosion Inhibitors for Steel in Hydrochloric Acid. *Portugaliae Electrochimica Acta*, **26**, 211-220 (2008).

57. Singh. A, Ansari. K. R, Haque. J, Dohare. P, Lgaz. H, Salghi. R, Quraishi. M. A. Effect of electron donating functional groups on corrosion inhibition of mild steel in hydrochloric acid: Experimental and quantum chemical study. *Journal of the Taiwan Institute of Chemical Engineers*, **82**, 233-251 (2018).

استخدام الميكروويف في تحضير بعض مرتبطات قاعدة شيف من مشتقات الترايازول ومتراكباتها وتوصيفها وتقييمها من حيث نشاطها البيولوجي وكذلك كمثبطات للتآكل

علي مصطفى علي حسن[١]، باسم حسين هيكل[٢]، احمد يونس[٣]، محمود عبد المنصف جاد بدير[١]، زغلول ابراهيم البيلي[٤]، معتز محمد عبد السلام محمد[٤]

[١]كلية العلوم- جامعة الأزهر- القاهرة- مصر.
[٢]شركة القاهرة لتكرير البترول- مسطرد- القليبوبية- مصر.
[٣]المركز القومي للبحوث- الدقي- الجيزة- مصر.
[٤]الهيئة المصرية العامة للمواصفات والجودة- القاهرة- مصر.

استخدام الكيمياء الخضراء كطريقه جديده ومقتصدة في تحضير بعض المتراكبات لعناصر الكوبلت والنيكل النحاس والزنك مع المترابط (مشتق الترايازول) وذلك باستعمال الميكروويف، كما تم توصيف وإثبات المترابط و متراكباته باستخدام وسائل تحليل مختلفة مثل التحاليل العنصرية والقياسات الطيفيه الخاصه بالأشعه فوق البنفسجيه والأشعة تحت الحمراء والرنين النووي المغناطيسي ومطياف الكتلة والتحليل الحراري لمتراكبات الكوبلت والنيكل والنحاس والزنك كذلك تمت دراسة النشاط البيولوجي للمرتبطات ومقارنة نتائجها بمتراكبات الزنك ، وقد أظهرت المتراكبات أن لها تأثير مقبول كمضادات للبكتريا والفطريات مقارنة بالمرتبط.

كذلك تم دراسة وتقيم كفاءة المرتبطات المحضرة في مجال مثبطات التآكل حيث تم اجراء تجارب تعتمد على قياسات الفقد في الوزن في ثلاث درجات حرارة مختلفة باستخدام اقراص من الحديد الكربوني في بيئة حمضية تحتوي على ١ مولار من حمض الهيدروكلوريك، وقد اظهرت النتائج ان المرتبطات لها تأثير مقبول من حيث كونها مواد مثبطة للتآكل حيث اظهر المرتبط المحتوي على حلقة الثيوفين نتيجة افضل من المرتبط المحتوي على حلقة الفيوران.